

# Microfluidic Chip-Based Fabrication of PLGA Microfiber Scaffolds for Tissue Engineering

Chang Mo Hwang,<sup>†,‡</sup> Ali Khademhosseini,<sup>§,||</sup> Yongdoo Park,<sup>†,#</sup> Kyung Sun,<sup>†,⊥,#</sup> and Sang-Hoon Lee<sup>\*,⊥</sup>

Korea Artificial Organ Center, Department of Thoracic and Cardiovascular Surgery, and Department of Biomedical Engineering, College of Medicine, Korea University, Seoul 136-705, Republic of Korea, Harvard-MIT Division of Health Sciences and Technology, Massachusetts Institute of Technology, Cambridge, Massachusetts 02139, Center for Biomedical Engineering, Department of Medicine, Brigham and Women's Hospital, Harvard Medical School, Boston, Massachusetts 02115, and Department of Biomedical Engineering, College of Health Science, Korea University, Seoul 136-703, Republic of Korea

Received January 25, 2008. Revised Manuscript Received March 27, 2008

In this paper, we have developed a method to produce poly(lactic-co-glycolic acid) (PLGA) microfibers within a microfluidic chip for the generation of 3D tissue engineering scaffolds. The synthesis of PLGA fibers was achieved by using a polydimethylsiloxane (PDMS)-based microfluidic spinning device in which linear streams of PLGA dissolved in dimethyl sulfoxide (DMSO) were precipitated in a glycerol-containing water solution. By changing the flow rate of PLGA solution from 1 to 50  $\mu\text{L}/\text{min}$  with a sheath flow rate of 250 or 1000  $\mu\text{L}/\text{min}$ , fibers were formed with diameters that ranged from 20 to 230  $\mu\text{m}$ . The PLGA fibers were comprised of a dense outer surface and a highly porous interior. To evaluate the applicability of PLGA microfibers generated in this process as a cell culture scaffold, L929 fibroblasts were seeded on the PLGA fibers either as-fabricated or coated with fibronectin. L929 fibroblasts showed no significant difference in proliferation on both PLGA microfibers after 5 days of culture. As a test for application as nerve guide, neural progenitor cells were cultured and the neural axons elongated along the PLGA microfibers. Thus our experiments suggest that microfluidic chip-based PLGA microfiber fabrication may be useful for 3D cell culture tissue engineering applications.

## Introduction

Tissue engineering and regenerative medicine have generated a great deal of excitement as a method of generating engineered biological tissue substitutes for a wide range of diseases.<sup>1–5</sup> A key aspect of tissue engineering approaches is the development of scaffolds that support, stimulate, and direct the growth of specific cells. To generate a functional tissue engineering scaffold, biodegradable and biocompatible materials are required. In addition to the materials, cell proliferation and tissue formation are greatly affected by the physical properties of scaffolds, such as porosity, surface roughness, elasticity, and the three-dimensional (3D) architecture of the scaffold.<sup>3,6,7</sup> As in 3D morphologies, for example, small pores in the scaffold matrix have been shown to facilitate cell proliferation and the storage of nutrients and chemicals for specific functional roles by releasing cytokines for controlling cell growth or drugs to prevent

infection.<sup>8,9</sup> Moreover, the rate of degradation of a scaffold is influenced by the pore dimensions and overall shape of the scaffold.<sup>10–12</sup> Therefore, many technologies have been developed to create scaffolds with well-defined physical and architectural features. These techniques include salt or particulate leaching,<sup>8,10,12,13</sup> rapid prototyping,<sup>14</sup> self-assembled hydrogels,<sup>5,15</sup> electrospinning,<sup>12,16,17</sup> and phase separation.<sup>18</sup>

Fibrous scaffolds are of potential interest for tissue engineering since they can enable the guided cell growth, alignment, and migration. Fibers can be fabricated to 3D woven or nonwoven scaffold forms in sheet and tubular structure. Tissue engineering scaffolds are fabricated from biomaterials such as naturally occurring polymers such as chitosan, hyaluronic acid, silk,

\* Corresponding author. Tel: + 82-2-920-6457. Fax: +82-2-921-6818. E-mail: dbiomed@korea.ac.kr.

<sup>†</sup> Korea Artificial Organ Center, Korea University.

<sup>‡</sup> Department of Biomedical Engineering, College of Health Science, Korea University.

<sup>§</sup> Massachusetts Institute of Technology.

<sup>||</sup> Harvard Medical School.

<sup>#</sup> Department of Biomedical Engineering, College of Medicine, Korea University.

<sup>⊥</sup> Department of Thoracic and Cardiovascular Surgery, Korea University.

(1) Langer, R.; Vacanti, J. P. *Science* **1993**, *260*, 920–926.

(2) Vunjak-Novakovic, G.; Altman, G.; Horan, R.; Kaplan, D. L. *Annu. Rev. Biomed. Eng.* **2004**, *6*, 131–156.

(3) Vacanti, J. P.; Langer, R. *Lancet* **1999**, *354* Suppl 1, S132–34.

(4) Sarkar, S.; Dadhania, M.; Rourke, P.; Desai, T. A.; Wong, J. Y. *Acta Biomater.* **2005**, *1*, 93–100.

(5) Kim, J.; Kim, I. S.; Cho, T. H.; Lee, K. B.; Hwang, S. J.; Tae, G.; Noh, I.; Lee, S. H.; Park, Y.; Sun, K. *Biomaterials* **2007**, *28*, 1830–1837.

(6) Khademhosseini, A.; Langer, R.; Borenstein, J.; Vacanti, J. P. *Proc. Natl. Acad. Sci. U.S.A.* **2006**, *103*, 2480–2487.

(7) Cooper, J. A.; Lu, H. H.; Ko, F. K.; Freeman, J. W.; Laurencin, C. T. *Biomaterials* **2005**, *26*, 1523–1532.

(8) Kim, T. K.; Yoon, J. J.; Lee, D. S.; Park, T. G. *Biomaterials* **2006**, *27*, 152–159.

(9) Liang, D.; Hsiao, B. S.; Chu, B. *Adv. Drug Delivery Rev.* **2007**, *59*, 1392–1412.

(10) Oh, S. H.; Kang, S. G.; Lee, J. H. *J. Mater. Sci. Mater. Med.* **2006**, *17*, 131–137.

(11) Zong, X.; Bien, H.; Chung, C. Y.; Yin, L.; Fang, D.; Hsiao, B. S.; Chu, B.; Entcheva, E. *Biomaterials* **2005**, *26*, 5330–5338.

(12) Lee, Y. H.; Lee, J. H.; An, I. G.; Kim, C.; Lee, D. S.; Lee, Y. K.; Nam, J. D. *Biomaterials* **2005**, *26*, 3165–3172.

(13) Chevalier, E.; Chulia, D.; Pouget, C.; Viana, M. *J. Pharm. Sci.* **2007**, *97*, 1135–1154.

(14) Leong, K. F.; Cheah, C. M.; Chua, C. K. *Biomaterials* **2003**, *24*, 2363–2378.

(15) Fedorovich, N. E.; Alblas, J.; de Wijn, J. R.; Hennink, W. E.; Verbout, A. J.; Dhert, W. J. *Tissue Eng.* **2007**, *13*, 1905–1925.

(16) Bashur, C. A.; Dahlgren, L. A.; Goldstein, A. S. *Biomaterials* **2006**, *27*, 5681–5688.

(17) Fridrikh, S. V.; Yu, J. H.; Brenner, M. P.; Rutledge, G. C. *Phys. Rev. Lett.* **2003**, *90*, 144502.

(18) Smolders, C. A.; Reuvers, A. J.; Boom, R. M.; Wienk, I. M. *J. Membr. Sci.* **1992**, *73*, 259–275.

alginate, collagen,<sup>2,5,19,20</sup> and several synthetic biodegradable polymers.<sup>10–12,16,21</sup> PLGA is a well-known synthetic material that has been approved by the Food and Drug Administration for clinical applications. To date, several PLGA fiber fabrication methods, such as melt spinning, wet spinning, and electrospinning, have been developed.<sup>11,13,17,22,23</sup> Thermal processes like melt spinning and solid free-form manufacturing require bulky and heavy apparatuses.<sup>13</sup> Additionally, high temperatures limit protein loading for the controlled delivery of bioactive molecules to promote tissue formation. To generate thinner fibers, electrospinning methods have been widely applied in tissue regeneration.<sup>10,11,16,17,20</sup> However, the electrospinning process has difficulty manufacturing fibers in thick 3D structured scaffolds, because of nanofibrous characteristics.<sup>12,16,17</sup> In this paper, we describe a method of fabricating PLGA microfibers by using an “on the fly” phase inversion (liquid to solid) process by using a microfluidic system. This process is simple, cost-effective, and compatible with many biological materials and can be used to generate microlevel diameter (10 to several hundred micrometers) and uniform fibers in a reproducible and scalable manner. Furthermore, we developed a method to align the fabricated fibers with high directionality and investigated the feasibility of the resulting fibrous scaffold for guided tissue regeneration. L929 mouse fibroblast cells and rat neural progenitor cells were cultured on the fibers, and the cytocompatibility and morphology of the seeded cells were investigated.

## Materials and Methods

**Materials.** Poly(D,L-lactic-co-glycolic acid) (Resomer RG 504H, 50:50) random copolymer was purchased from Boehringer Ingelheim Pharma GmbH & Co. KG. This copolymer has an intrinsic viscosity of 0.45–0.60 dL/g in 0.1% CHCl<sub>3</sub>. PDMS (Sylgard 184) was obtained from Dow Corning. DMSO (purity 99%), glutaraldehyde (25% aqueous solution), and glycerol anhydrous (purity 98%) were purchased from Fluka, and *tert*-butyl alcohol (purity 98%) was purchased from Junsei. Hanks’ balanced salt solution (HBSS) and Dulbecco’s modified Eagle medium (DMEM) were purchased from Gibco Laboratories. For immunofluorescence, Alexa Fluor 568 phalloidin, Alexa Fluor 488, 4’,6-diamidino-2’-phenylindole dihydrochloride (DAPI), and Prolong Gold antifade reagent were purchased from Invitrogen. Cell proliferation reagent WST-1 was purchased from Roche Applied Science.

**PLGA Fiber Fabrication.** The microfluidic-based fabrication apparatus and procedure of the non-PLGA microfibers (e.g., 4-hydroxybutyl acrylate and alginate) have been previously reported.<sup>19,24,25</sup> We used a modified setup comprised of the microfluidic system and a fiber winding system as shown in Figure 1a. The end of a core pipet (30 μm in inner diameter) was cut and ground smoothly using a microforge (MF-900, Narishige). The core solution (10% PLGA in DMSO) and sheath solution [mixture of glycerin and distilled water with 50% (v/v)] were introduced into each inlet, respectively. The schematic of PLGA fiber generation is illustrated in Figure 1b. At the position where the two fluids merged (around the dotted rectangle of Figure 1a), the sheath fluid surrounded the tip of the core glass while the core fluid extruded through the core

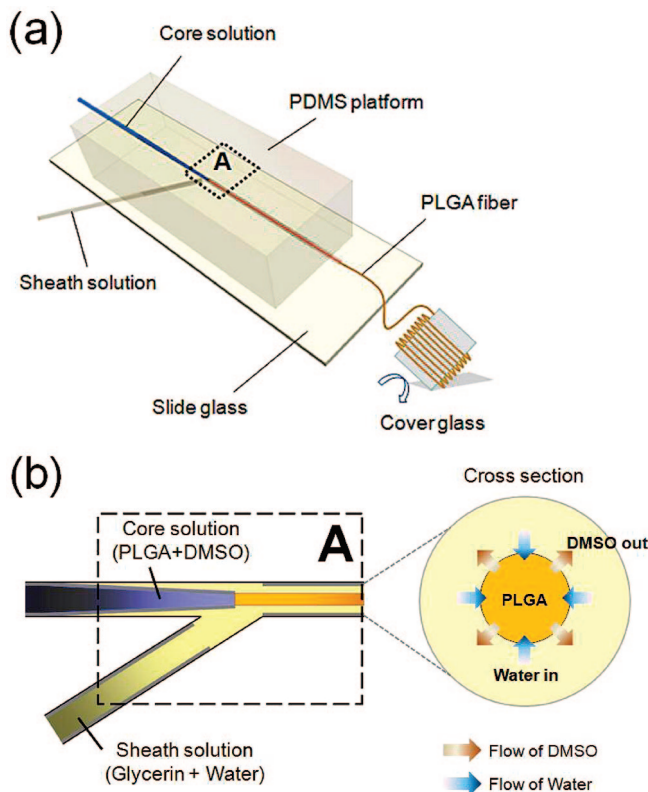


**Figure 1.** (a) Schematic of a microfluidic chip and a cover glass winding device for the aligned PLGA fibers. (b) Principle of the phase inversion process during polymer precipitation.

glass to form a stable coaxial flow because of microfluidic phenomena. At the interface between the core PLGA solution and sheath fluid, the exchange of DMSO and water occurs and the polymer in the liquid phase solution is solidified.<sup>18,26,27</sup>

The diameter of PLGA fibers was controlled by regulating the core flow rate at 1, 2, 5, 10, 20, or 50 μL/min under two sheath fluid flow rates (250 and 1000 μL/min). The extruded PLGA fibers were immersed in a water bath for further precipitation. The aligned bundle of fiber was made by winding the nascent fibers on a cover glass (18 × 18 mm). To measure the fiber diameter, 40 samples (from 10 images) were measured per each flow condition with a microscope (Zeiss Axiovert 200M, Carl Zeiss, Germany) and AxioVision LE 4.5 software. For cell culture, the scaffold was prepared and subsequently (1) immersed in distilled water for 24 h to remove residual DMSO, (2) sterilized with 70% ethanol overnight, (3) rinsed three times with distilled water for 3 min, and (4) stored in PBS with penicillin (100 units/mL) and streptomycin sulfate (100 μg/mL).

**Protein Incorporation.** With the same DMSO solvent, 10 and 20 wt % PLGA solutions were prepared, 5 μL of aqueous protein solution (2 mg/mL) was added to 1 mL of PLGA solution, and they were mixed well with a vortex mixer. For the convenience of confirming the protein incorporation, we used antibody labeled with fluorescence (Alexa Fluor 488, goat anti-mouse IgG), and the spun fibers were examined with a fluorescence microscope.

For testing in vitro protein release, high concentration protein incorporated PLGA solution (50 μL of protein per 1 mL of PLGA solution) was used with three samples for each concentration. Protein release samples were spun for 3 min, collected, immediately soaked with distilled water for 3 min, and moved to 12-well plates. Each well was filled with 3 mL of distilled water and reserved in an incubator with 37 °C, 95% humidity. After a predetermined time (15, 30 min, 1, 2, 4, 30 h), absorbance at 568 nm was measured with a spectrophotometer (Optizen 3220UV, Microsyst).

(26) Strathmann, H.; Kock, K. *Desalination* **1977**, *21*, 241–255.

(27) Mulder, M. *Basic Principles of Membrane Technology*; Kluwer Academic Publishers: Dordrecht, 1996.

(19) Shin, S. J.; Park, J. Y.; Lee, J. Y.; Park, H.; Park, Y. D.; Lee, K. B.; Whang, C. M.; Lee, S. H. *Langmuir* **2007**, *23*, 9104–9108.

(20) Tian, F.; Hosseinkhani, H.; Hosseinkhani, M.; Khademhosseini, A.; Yokoyama, Y.; Estrada, G. G.; Kobayashi, H. *J. Biomed. Mater. Res.* **2008**, *84A*, 291–299.

(21) Oh, S. H.; Park, I. K.; Kim, J. M.; Lee, J. H. *Biomaterials* **2007**, *28*, 1664–1671.

(22) Smeal, R. M.; Rabbitt, R.; Biran, R.; Tresco, P. A. *Ann. Biomed. Eng.* **2005**, *33*, 376–382.

(23) Williamson, M. R.; Adams, E. F.; Coombes, A. G. *Biomaterials* **2006**, *27*, 1019–1026.

(24) Oh, H. J.; Kim, S. H.; Baek, J. Y.; Seong, G. H.; Lee, S. H. *J. Micromech. Microeng.* **2006**, *16*, 285–291.

(25) Jeong, W.; Kim, J.; Kim, S.; Lee, S.; Mensing, G.; Beebe, D. J. *Lab Chip* **2004**, *4*, 576–580.

**Mouse Fibroblast and Neural Progenitor Cell Culture.** To evaluate the cytocompatibility of the PLGA fiber scaffold, prefabricated scaffolds were seeded with L929 mouse fibroblasts and rat primary neural progenitor cells. All PLGA scaffolds were dried and sterilized with ethylene oxide gas before cell seeding. L929 cells were cultured in DMEM with 10% fetal bovine serum, penicillin (100 units/mL), and streptomycin sulfate (100  $\mu\text{g}/\text{mL}$ ). The fibronectin-coated and noncoated PLGA fibers were prewetted with cell culture medium for 1 h prior to cell seeding to allow for the full diffusion of culture medium into the fiber pores. To adsorb fibronectin on to the scaffolds, fibers were dipped in a PBS-containing fibronectin (20  $\mu\text{g}/\text{mL}$ ) for 1 h and subsequently rinsed with PBS (three times for 3 min) to remove nonadsorbed proteins. L929 cells were seeded on the PLGA scaffolds at a density of  $10^5$  cells per scaffold. After 2 and 5 days in culture, mitochondrial activity was measured with a WST-1 proliferation kit ( $n = 6$ ).

To culture neural progenitor cells, cerebral cortices were harvested from the embryos of E18 Sprague–Dawley rats. Their meninges were removed, dissociated in calcium- and magnesium-free HBSS, and filtered in a 40  $\mu\text{m}$  nylon cell strainer (BD Bioscience) and analyzed for cell viability by using trypan blue staining. All animals were handled in accordance with the Guidelines of Korea University Hospital for Laboratory Animal Studies. To visualize the cells, each scaffold was seeded with  $10^5$  cells and supplied with neurobasal medium including B27 supplement, penicillin (100 units/mL), and streptomycin sulfate (100  $\mu\text{g}/\text{mL}$ ). To ensure the proper supply of nutrients, the culture medium was changed every 2 days. After 5 days in culture, cells were fixed, dehydrated, and lyophilized prior to analysis using SEM.

**Investigation of Cell Alignment.** To analyze the effects of fiber diameter on cell alignment, PLGA fibers that were 20, 50, and 80  $\mu\text{m}$  in diameter were prepared on a coverslip, seeded with  $10^5$  L929 cells, and cultured for 3 days ( $n = 4$ ). For the quantitative measurement of cell alignment, the deviation angles, which are defined as the angle between the elongated direction of cell and the longitudinal direction of fiber, were measured for 80 cells per each condition. The deviation angles were measured from SEM images for cells that crossed the centerline of the fibers.

**Actin Filament and Nuclear Staining of L929 Fibroblasts.** L929 fibroblast cells were stained for actin filaments and nuclei with Alexa Fluor 568 phalloidin and DAPI, respectively. For actin staining, cells were gently rinsed with PBS, fixed with 4% paraformaldehyde solution for 1 h under 37  $^{\circ}\text{C}$ , and then permeabilized with 1% Triton X-100 in PBS solution. Blocking was achieved using 3% bovine serum albumin (BSA) in PBS solution for 30 min. Actin filaments were stained with Alexa Fluor 568 phalloidin in PBS (1:40) including 1% BSA and reacted for 1 h. During the nuclear staining stage, DAPI stock solution (1 mg/mL) was diluted in distilled water (1:1000) and reacted for 5 min. Finally, to preserve fluorescence, all samples were coated with Prolong Gold antifade reagent.

**Scanning Electron Microscopy.** The scaffolds were washed with PBS to remove nonadherent cells and then fixed with 2.5% glutaraldehyde for 2 h at room temperature. After rinsing twice with PBS for 5 min, the samples were treated with a 1% osmium tetroxide ( $\text{OsO}_4$ ) solution for 60 min. The samples were dehydrated through a series of graded ethanol washes for 20 min each at 50, 70, 80, 90, 95, and 100%. The ethanol was exchanged for *tert*-butyl alcohol, and the scaffolds were then freeze-dried with Maxi-Dry Lyo (Heto Holten). The cell cultured scaffolds were then sputter-coated with platinum at a pressure of 100 mTorr for 6 min. In the noncultured, bare PLGA scaffold samples, glutaraldehyde and  $\text{OsO}_4$  fixation processes were omitted. A field emission scanning electron microscope (FE-SEM) (Hitachi, S4700) was used to visualize the scaffolds.

## Results and Discussion

**Fabrication of PLGA Fibers within Microchannels.** PLGA microfibers were produced by using a phase inversion process to precipitate a stream of PLGA in DMSO within a microfluidic chip. Figure 2a illustrates the fiber extrusion at the end of the

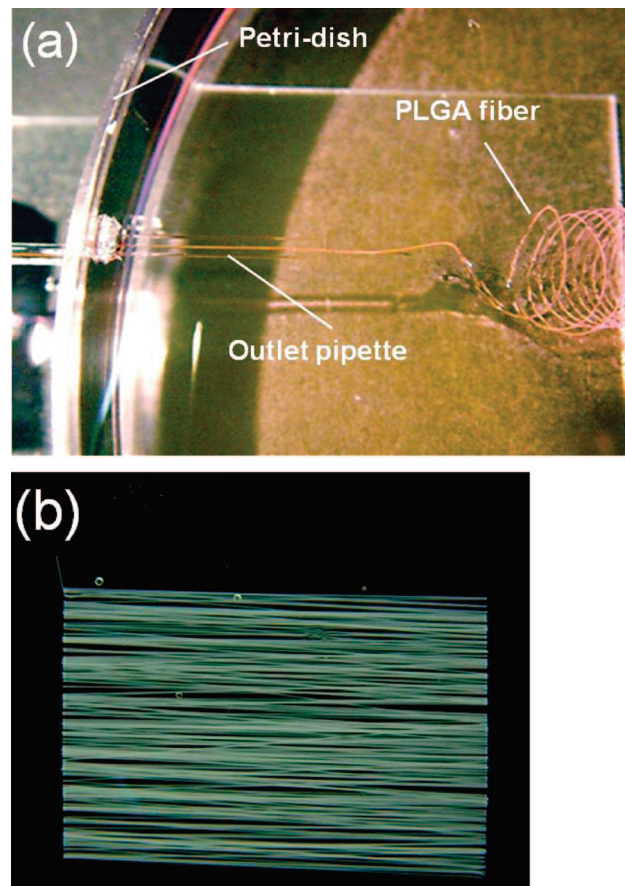


**Figure 2.** PLGA spinning with a microfluidic chip. (a) Fiber generation with the chip and (b) PLGA fiber scaffold for cell culture wound around a coverslip (18  $\times$  18 mm) during spinning (at 60 rpm).

outlet pipet. The PLGA solution in the core pipet maintained its liquid state before contact with sheath fluid and precipitated upon exposure to the nonsolvent at the outlet pipet. The initial precipitation time of the PLGA fiber in the outlet pipet was rapid ( $< 250$  ms). As expected, the fiber production rate was dependent on the core and sheath flow rates. For example, the fiber spinning rate was approximately 40 mm/s for the core flow rate of 5  $\mu\text{L}/\text{min}$  and a sheath flow rate of 1000  $\mu\text{L}/\text{min}$ . The fiber generation speed can be increased by simply increasing the core and sheath flow rates, thus demonstrating the advantage of this process for the mass production of PLGA fibers. Figure 2b shows the fabrication of aligned fibers by winding the extruded fibers on a rotating coverslip at 60 rpm speed (see Figure S1 of the Supporting Information for demonstrating PLGA fiber spinning with a winding device). The key advantages of microfluidic fiber generation system are the versatility of size, little limitation in fiber length by continuous spinning, and protein or drug incorporation. As shown in Figure 3, the fiber size is controllable from 20 to 200  $\mu\text{m}$ , with highly uniform diameter distribution along the fiber and less than 5% variation in diameter. This fabrication process is simple, cost-effective, and compatible with many biological materials, since microfibers can be formed without heat, high pressures, or toxic chemicals. In addition, this method facilitates the generation of thin ( $< 25$   $\mu\text{m}$ ) and uniform fibers in a reproducible and scalable manner and it can be easily modified to control the fiber size simply by controlling the flow rate. In addition, it is anticipated that the procedure is widely applicable to other materials with various cross-linking mechanisms, such as photopolymerization (e.g., polyethyleneglycol

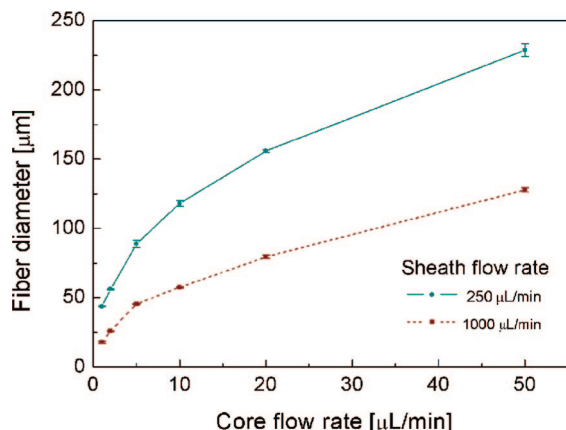


**Figure 3.** PLGA fiber diameter with various core flow rates under sheath flow rates of 250 and 1000  $\mu\text{L}/\text{min}$  ( $n = 40$ , mean  $\pm$  SD).

diacrylate, 4-hydroxybutyl acrylate),<sup>24,25</sup> ionic gelation (e.g., alginate),<sup>19</sup> and thermal phase transition (e.g., agar).<sup>2,6</sup>

**Morphology of the PLGA Microfiber.** To study the ability to change the diameter of the resulting PLGA microfibers, we investigated the effects of changing the sheath and core fluid flow rates. It was observed that by controlling the sheath (250 and 1000  $\mu\text{L}/\text{min}$ ) and core flow rates (1, 2, 5, 10, 20, 50  $\mu\text{L}/\text{min}$ ) PLGA fibers could be obtained with diameters that increased,<sup>26</sup> and the resulting fiber diameters also increased. Furthermore, as the sheath flow rate increased, the diameter of the fibers decreased. This is expected, since the increasing the sheath flow rate will result in increased shearing and stretching of the core fluid. In this experiment, when the tip diameter is 30  $\mu\text{m}$ , the minimum fiber diameter is around 20  $\mu\text{m}$  under this sheath/core fluid condition. When we change the flow condition, the fiber diameter may be reduced, but the fibers were not handled easily. If we want to obtain a smaller fiber, then we may change either the glass tip to a smaller diameter or the winding speed, but the latter sometimes results in irregular fiber diameter and disconnection.

To analyze the morphology of the PLGA fibers, we used the fibers from SEM images shown in Figure 4a. It was found that the PLGA fibers were cylindrical in shape with uniform diameters and a smooth surface. The cross-sectional images of the PLGA fibers showed the presence of three distinct regions comprising a dense skin layer as well as a middle and center region each of which contained a macrovoid. The skin layer comprised a dense polymeric structure that was a few microns in thickness. The central region consisted of irregular, large, elongated voids, while the middle region contained smaller voids. These structures are formed by a diffusion-controlled process of the water (nonsolvent)<sup>23,26,27</sup> and a schematic explaining the mechanism of void-formation is illustrated in Figure 1b. At the interface between the core PLGA solution and sheath fluid, the rapid exchange of DMSO and water occurs by short-range diffusion and the dense skin layer is formed. But, this dense skin layer decreases the subsequent water and DMSO diffusion. Therefore, the PLGA precipitation at the middle region occurs more slowly than at the interface and middle-sized voids are formed. Similarly, the larger voids are created at the central region because of the slower diffusion between water and DMSO.

**Protein Loading and Release.** Protein-incorporated fibers under a fluorescence microscope is shown in Figure 5a, which reflects that the protein was evenly incorporated in the PLGA fibers. Other several types of cytokines or peptides are soluble in DMSO, and they can be easily loaded in the PLGA fibers through the wet spinning process. If a protein of interest has poor solubility in organic solvents, this hurdle can be circumvented

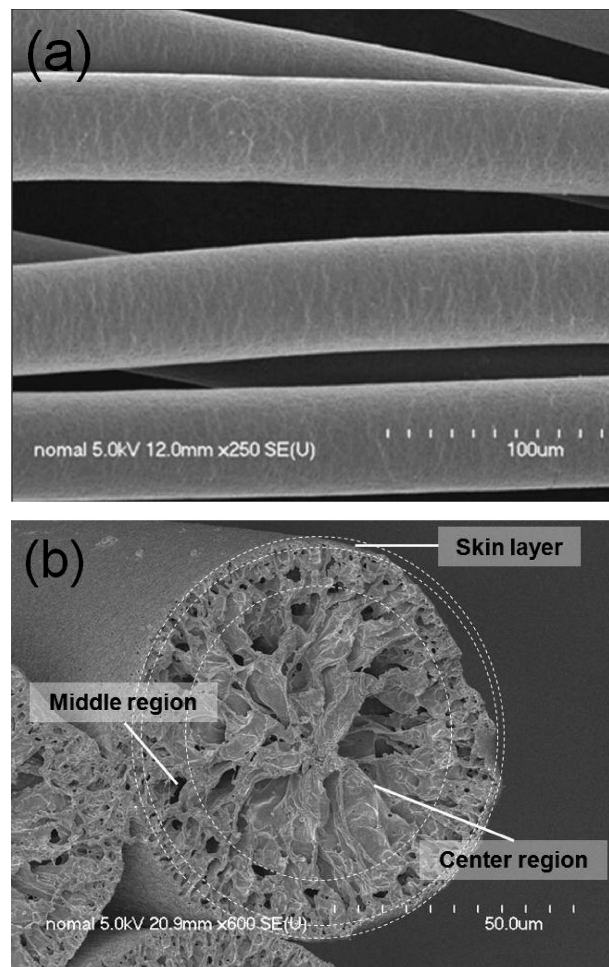


**Figure 4.** SEM micrograph of PLGA microfibers. (a) Surface of PLGA fibers. Scale bar is 100  $\mu\text{m}$ . (b) Cross sectional view of a fiber. Scale bar is 50  $\mu\text{m}$ .

by adding a premixing step such as the water in oil solvent evaporation method.<sup>8,28</sup>

The release profile of protein concentration in the solution is shown in Figure 5b, and the cumulative release profile reflects the saturation state after about 30 h. This profile shows the feasibility of incorporation and release of protein in the PLGA fibers. It is anticipated that the inner microvoids can be used as a reservoir for cytokines or proteins that promote cell adhesion and growth; nutrients and cell growth factors stored in the voids can diffuse through the thin skin layer and be delivered to cells.

**L929 Fibroblast Culture on the PLGA Fiber.** L929 fibroblast cells were cultured on the surface of bare PLGA and fibronectin-coated PLGA fibers. Figure 6a illustrates an F-actin stained image of fibroblast cells cultured for 48 h on noncoated PLGA fiber. Actin (red) and nuclear (blue) fluorescence with bright field image of PLGA fibers are clearly observed. The proliferation of cultured cells on the fibronectin-coated and noncoated PLGA fibers was evaluated by measuring mitochondrial activity through the use of a cell proliferation reagent WST-1 kit as shown in Figure 6b. No significant difference was observed between the two groups after 2 days in culture. However after 5 days in culture an increase of absorbance in the both group was detectable ( $n = 6$ ,  $p < 0.01$  each group). It is well-known that fibronectin is a cell binding adhesive protein in extracellular matrices<sup>6,16,23,29,30</sup> and a

(28) Chew, S. Y.; Wen, J.; Yim, E. K.; Leong, K. W. *Biomacromolecules* 2005, 6, 2017–2024.

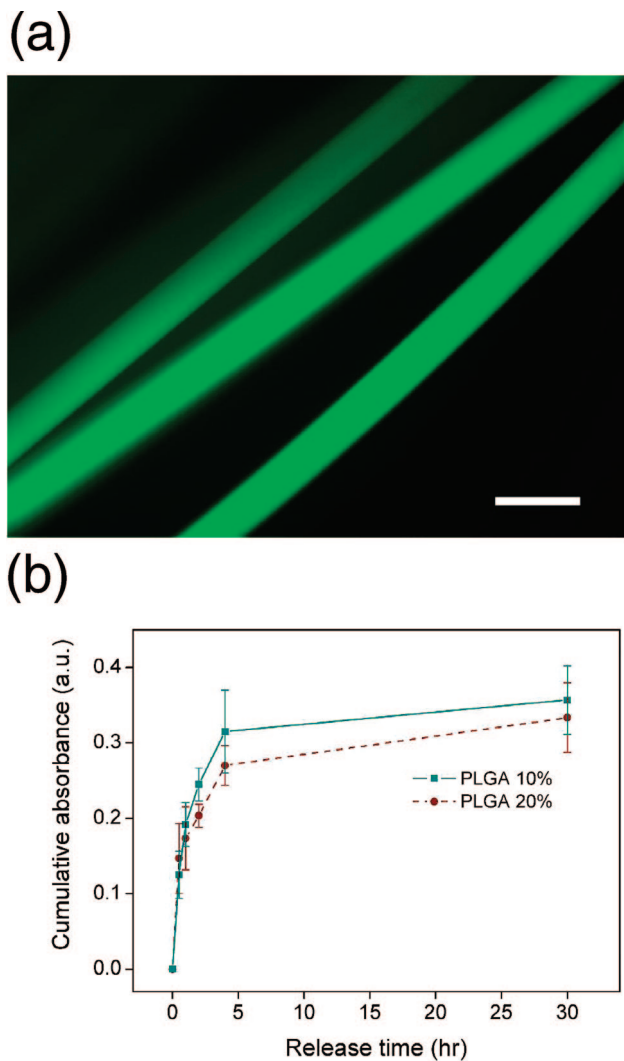


**Figure 5.** Protein incorporation in PLGA fibers and release test. (a) Protein-incorporated PLGA fibers under a fluorescence microscope. Scale bar is 100  $\mu\text{m}$ . (b) Cumulative release profile of protein ( $n = 5$ , mean  $\pm$  SD) (au: arbitrary unit).

fibronectin coating is used to improve cell attachment. This result shows that untreated PLGA fibers were not significantly different in cell proliferation compared with fibronectin-coated fibers, indicating that the cytocompatibility of untreated PLGA fibers was comparable to that of fibronectin-coated samples.

**Analysis of Cell Alignment.** To assess the effects of cell alignment as a function of fiber diameter, we analyzed the morphological changes of L929 cells on PLGA fibers in vitro. We have quantitatively measured the orientation of cells cultured on the fibronectin-coated fibers by using image analyzing software (AxioVision LE 4.5). Figure 7a,b illustrates the SEM images of cells on the fibronectin-coated PLGA fibers (diameter, 20, 80  $\mu\text{m}$ ). As can be seen, most cells aligned along the axial direction of the fiber after 3 days of culture.

Cells on the larger fibronectin-coated PLGA fibers (diameter: 80 $\mu\text{m}$ ) did not exhibit these preferred orientations. This figure clearly indicates that the L929 cells tend to align well along the longitudinal direction as the fibers become thinner.

The deviation angles on cells cultured on PLGA fibers were quantitatively measured and are plotted in Figure 7c. For 20  $\mu\text{m}$

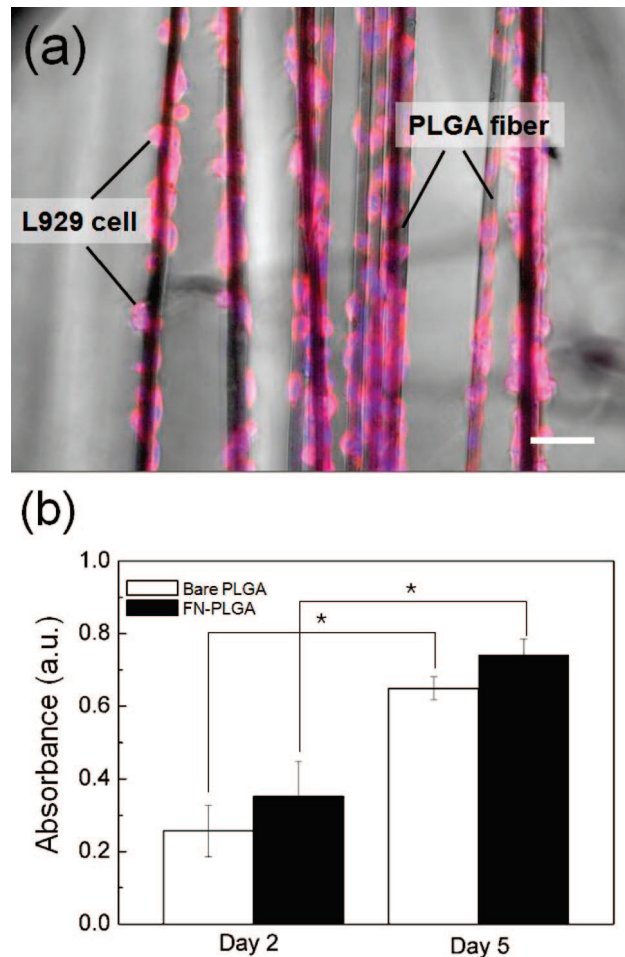


**Figure 6.** Results of L929 cells seeded on PLGA fiber scaffolds. (a) F-actin staining of fibroblast cells cultured for 48 h. Actin (red) and nuclear (blue) fluorescence-stained L929 fibroblasts with bright field image of PLGA fibers with no coating. Scale bar is 50  $\mu\text{m}$ . (b) WST-1 results of 2 and 5 days culture ( $n = 6$ ,  $*p < 0.01$ ). There is a significant difference between 2 days and 5 days culture in both the noncoated and the fibronectin (FN) coated groups.

fibers, the mean deviation angle was less than 10 $^\circ$  with small error bars. When the diameter was greater 80  $\mu\text{m}$ , their directionality was nearly random, similar to cells cultured on flat Petri dishes (data not shown). These results indicate that the cell alignment is closely related with the diameter of fibers. For tissue engineering applications in which cellular orientation is beneficial, as in neural cell culture, the ability to generate fibers in which cells can orient is a potentially useful advantage.

To date, cell alignment on a two-dimensional substrate has been reported by several groups by using microcontact printing of proteins,<sup>6,15,31</sup> microgrooved structures,<sup>4</sup> and nanofibers.<sup>9,11,16,20,28</sup> Despite their usefulness in controlling cell morphology, cell alignment with microfibers has a number of advantages in comparison to two-dimensional substrates.<sup>7,22,23,30</sup>

These advantages are (1) 3D-structured scaffolds of microfibers provide a more well defined environment than a 2D scaffold; (2) microfibers are easy to handle and can be easily surface modified, and (3) scaffolds are easily fabricated and can be readily implanted for therapeutic applications. In spite of these benefits, cultures of cells aligned on microfibers have not gained popularity due both to the difficulty in fabricating diverse microsized PLGA fibers in a simple, cost-effective way and the difficulty in handling

(29) Ostrovidov, S.; Jiang, J.; Sakai, Y.; Fujii, T. *Biomed. Microdevices* **2004**, *6*, 279–287.

(30) Lietz, M.; Dreesmann, L.; Hoss, M.; Oberhoffner, S.; Schlosshauer, B. *Biomaterials* **2006**, *27*, 1425–1436.

(31) Tien, J.; Nelson, C. M.; Chen, C. S. *Proc. Natl. Acad. Sci. U.S.A.* **2002**, *99*, 1758–1762.

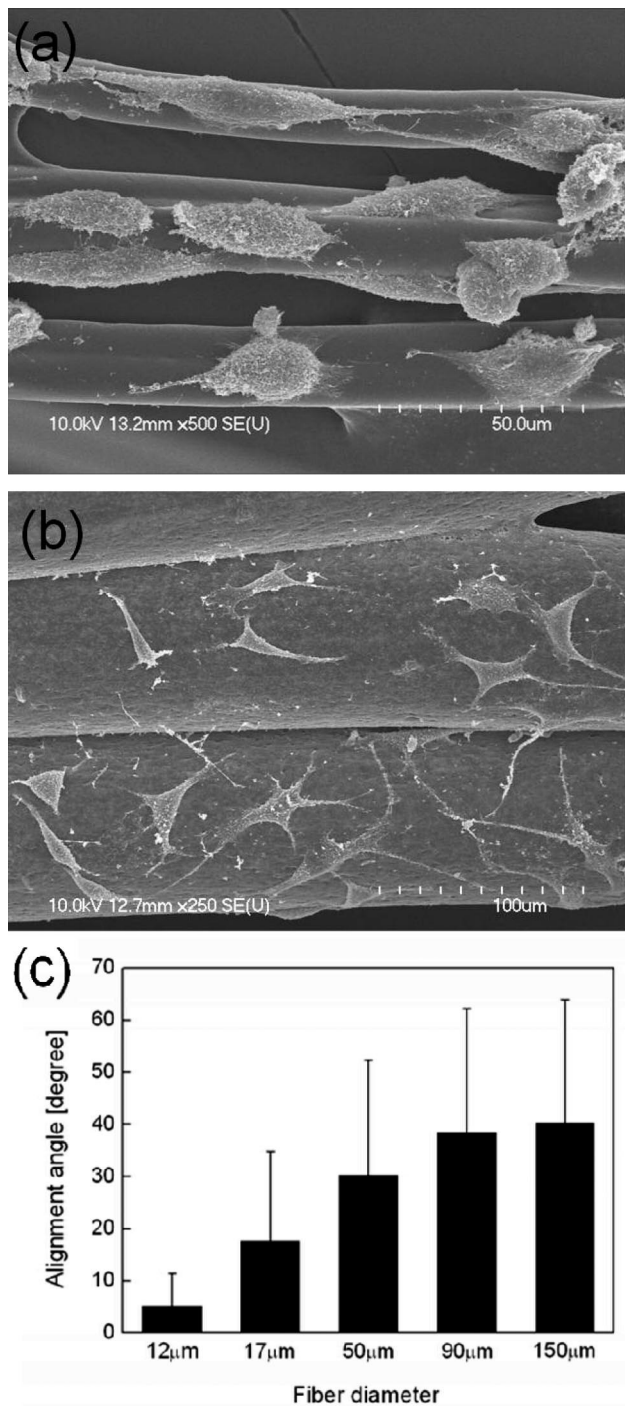


**Figure 7.** L929 cell alignment along the longitudinal direction on FN-coated PLGA fibers: (a) diameter of 20 μm (scale bar is 50 μm) and (b) diameter of 80 μm (scale bar is 100 μm). (c) Cell orientation according to the fibers' diameter ( $n = 80$  each, mean  $\pm$  SD).

such fibers. Our method fabricating PLGA microfibers using a microfluidic chip and our technique of aligning these fibers by winding them on glass provides a simple approach that can overcome many limitations of the existing technologies for fabricating PLGA scaffolds.

**Neuronal Cell Culture on PLGA Fibers.** For the feasibility of PLGA microfibers for neural tissue engineering, primary neuronal cells were seeded on PLGA scaffolds (diameter, 25 μm) to examine the guided growth of neurites. Neuronal cells that were seeded on bare PLGA fibers extended their neurites, which extended to several hundred micrometers after 5 days of

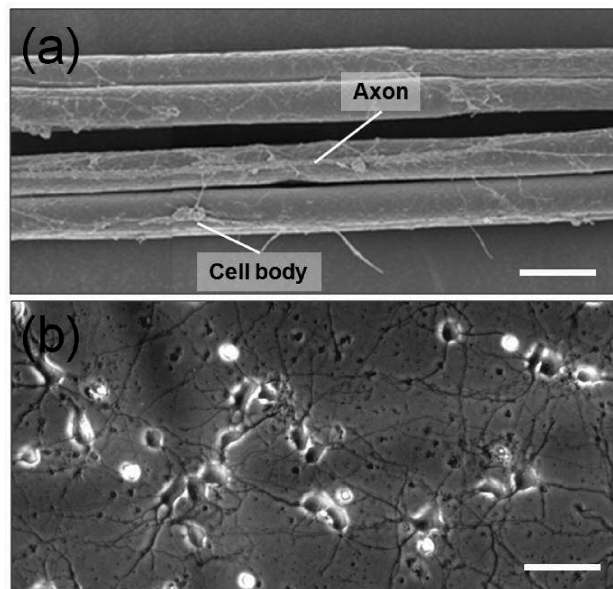


**Figure 8.** (a) SEM image of neural cells on the PLGA fibers and (b) neural cells cultured on a Petri dish for 3 days. Scale bars are 50 μm.

culture in vitro. As shown in Figure 8a, neurites aligned parallel to the fibers' orientation. Figure 8b shows an image of neural cells cultured on Petri dish for 5 days and indicates that neural cells grew randomly on the planar surface. Neuronal cell attachment and guided growth of neurites on the surface of PLGA fibers suggest the potential application of the PLGA microfibers for neural tissue engineering and spinal cord regeneration.<sup>22,28,30</sup>

#### Impacts of the Presented Microfiber Generation Technology.

In this paper, we showed the aligned cell-loaded fibers which mimic real tissues where the cells are aligned in parallel manners; cell alignment is essential for tissue constructs, such as ligament and tendon (collagen type I, III from fibroblasts),<sup>2,7</sup> heart muscles,<sup>11</sup> and spinal cord or neural tissues (axons from neurons).<sup>22,30,32</sup> After a sufficient time for cell proliferation, the parallel wound fibers could also show high density cell constructs, implying potential ability for tissue regeneration; the fibroblasts cultured for 10 days covered the PGLA fibers and formed a three-dimensional configuration (see Figure S2 of the Supporting Information). The resulting microfibers are appropriate for tissue engineering because (1) they give room for cell ingrowth, (2) it is possible to incorporate proteins or cytokines and sustained release,<sup>28</sup> and (3) it provides the technology for researchers to make various forms of 3D scaffolds.

In tissue engineered scaffolds, the space for cell ingrowth and proliferation is essential in regeneration of three-dimensional tissue constructs.<sup>1,3</sup> However, the fibers and membranes prepared by the electrospinning process do not support some of these requirements. The electrospun fibers are as small as 10 nm to 10 μm in diameter,<sup>16,17,20,28</sup> which can give environments for cell alignment on the surface of electrospun polymer webs and sufficient porosity for nutrients and metabolic wastes to pass through the membranes. However, apart from fiber diameter, electrospun membranes have nanolevel pore size which ranges from 10 to 1000 nm,<sup>12</sup> in which the cells cannot survive; the typical cell size, for example, of fibroblasts and osteoblasts is approximately 10 μm and increases to 50 μm when flattened.<sup>12,17</sup> Consequently, electrospun membranes cannot serve as scaffolds

(32) Thompson, D. M.; Buettner, H. M. *Ann. Biomed. Eng.* **2006**, *34*, 161–168.

for cell in growth, and only recently, an alternative try has been made to overcome this pore size insufficiency for tissue formation.<sup>12</sup> In contrast, the microfibers fabricated in the present study has a diameter range from 10 to 200  $\mu\text{m}$ , which can provide sufficient space in layered structure and woven/nonwoven forms. In addition, microfluidic chip-based microfibers can incorporate proteins such as growth factors, antibody, and cell adhesion peptides.

### Conclusion

In this study, we describe the microfluidic-based generation and alignment of PLGA microfibers by using a phase inversion process. Furthermore, we demonstrate the use of PLGA microfibers for 3D guided cell growth. The size of the fibers was easily controllable by changing the core and sheath fluid flow rates. This chip-based fabrication method has several advantages over conventional techniques: (1) the fabrication apparatus is simple, the chip is small, and the resulting fiber size can be easily controlled by varying flow conditions, and (2) the fabrication process does not require specific conditions, such as high temperatures or pressures, and sensitive biological materials like

proteins may be easily incorporated in the resulting fibers. Both fibroblasts and neural progenitor cells aligned along the longitudinal direction of the PLGA fibers. Through this study, we have demonstrated the emerging application of a microfluidic chip in the fabrication of fiber-based scaffolds for directional cell growth. It is anticipated that more complicated shaped scaffold can be fabricated by generating advanced winding methods. Such PLGA microfiber scaffolds could be applied to versatile applications such as scaffolds for neural tissue engineering.

**Acknowledgment.** This study was supported by a grant from NRL (National Research Lab) program, the Korea Science and Engineering Foundation (KOSEF), Republic of Korea (Grant No. R0A-2007-000-20086-0), and Ministry of Health & Welfare, Republic of Korea (Grant No. A020609).

**Supporting Information Available:** A figure demonstrating PLGA fiber spinning with a winding device (Figure S1) and an SEM image of 3D cell configuration at 10 days culture (Figure S2). This material is available free of charge via the Internet at <http://pubs.acs.org>.

LA800253B